

# Tunable Temperature-Responsive Supramolecular Hydrogels Formed by Prodrugs As a Codelivery System

Wei Ha, Jing Yu, Xin-yue Song, Juan Chen, and Yan-ping Shi\*

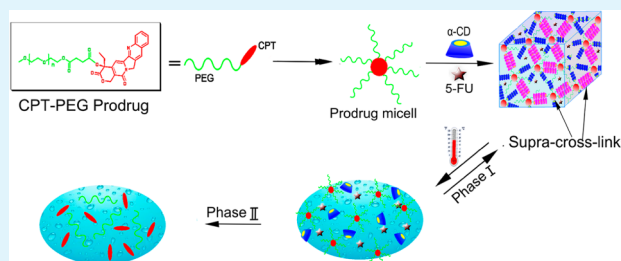
Key Laboratory of Chemistry of Northwestern Plant Resources of CAS and Key Laboratory for Natural Medicine of Gansu Province, Lanzhou Institute of Chemical Physics, Chinese Academy of Sciences, Lanzhou 730000, P. R. China

## Supporting Information

**ABSTRACT:** Taking advantage of the strong hydrophobicity of the anticancer drug camptothecin (CPT), the CPT molecule was conjugated to a class of low-molecular-weight (MW) poly(ethylene glycol) (PEG) chains (MW = 500, 1000, and 2000), forming an amphiphilic prodrug. The CPT-PEG prodrug formed stable hydrogels based on a combination of the partial inclusion complexation between one end of the PEG blocks and  $\alpha$ -CD and the hydrophobic aggregation of CPT groups. Meanwhile, the formed hydrogels could be loaded with water-soluble drug 5-fluorouracil (5-FU), which is always combined with CPT drugs to enhance their anticancer activity. Moreover, the hydrogel systems demonstrate unique structure-related reversible gel–sol transition properties at a certain temperature due to the reversible supramolecular assembly, and the gel–sol transition temperature could be modulated by varying the length of the PEG chain and the concentrations of  $\alpha$ -CD, demonstrating the possibility of achieving on-demand gel–sol transitions. The structure-related reversible gel–sol transition properties were proved by rheological property, XRD, DSC, and SEM measurements. The different controlled release profiles of two different anticancer drugs showed significant temperature-dependent properties. This easily prepared supramolecular hydrogel with excellent biocompatibility and tunable temperature responsiveness has significant potential for controlled drug release applications.

Moreover, the hydrogel systems demonstrate unique structure-related reversible gel–sol transition properties at a certain temperature due to the reversible supramolecular assembly, and the gel–sol transition temperature could be modulated by varying the length of the PEG chain and the concentrations of  $\alpha$ -CD, demonstrating the possibility of achieving on-demand gel–sol transitions. The structure-related reversible gel–sol transition properties were proved by rheological property, XRD, DSC, and SEM measurements. The different controlled release profiles of two different anticancer drugs showed significant temperature-dependent properties. This easily prepared supramolecular hydrogel with excellent biocompatibility and tunable temperature responsiveness has significant potential for controlled drug release applications.

**KEYWORDS:** temperature-sensitive hydrogels, tunable, host–guest inclusion, drug combination, codelivery system



## INTRODUCTION

Reversibility and responsiveness are ubiquitous in nature, whereby biological systems utilize stimuli-responsive aggregates to develop highly complicated and ordered materials.<sup>1</sup> The realization of reversibility and responsiveness for materials, especially for drug delivery materials, has received considerable attention in the improvement of properties and the development of new materials for site-specific drug delivery applications.<sup>2–6</sup> Various environment-sensitive materials that respond to an internal stimulus (e.g., pH, glucose, redox potential, and lysosomal enzymes) or external stimulus (e.g., temperature, magnetic field, ultrasound, and light) have been actively developed to accomplish site-specific drug release.<sup>7–14</sup> Hydrogels are water-swollen polymeric networks with broadly modifiable characteristics that enable wide utility in, for example, coatings, cosmetics, drug delivery, tissue engineering, and sensing applications.<sup>15–21</sup> Reversible and stimuli-responsive hydrogels have demonstrated great promise for site-specific drug delivery applications, as they can exhibit a sol–gel or gel–sol transition in response to external stimuli. Temperature is one of the most widely used stimuli for preparing stimuli-responsive hydrogels, since it is easy to control and has practical advantages both *in vitro* and *in vivo*.<sup>22,23</sup> Temperature-sensitive hydrogels have been extensively explored based on temperature-sensitive polymers or various temperature-responsive noncovalent interactions, such as host–guest interactions,

hydrogen bonds,  $\pi$ – $\pi$  stacking interaction, and so on.<sup>24–26</sup> Obviously, tunable temperature responses would generate more flexibility to further the applications of the hydrogels, and such hydrogels would provide the possibility of achieving on-demand gel–sol transition in many technological applications including biomedical ones. The ability to tune the temperature responsive gel–sol transition behavior of hydrogels in response to different temperatures is of significance not only to scientific research but also to potential applications. However, to date, there have only been a few reports in the literature on tunable temperature-responsive supramolecular hydrogels.<sup>27–29</sup>

Supramolecular gels constructed from low molecular weight molecules by reversible noncovalent interactions are a kind of adaptive material that can be sensitive to the environmental stimuli. Being responsive to multiple stimuli, these supramolecular gels are expected to be highly advantageous over traditional polymer gels and possess many unique properties that play a significant role in drug delivery systems.<sup>30–34</sup> Cyclodextrins (CDs) have successfully been exploited to design and form self-assembled hydrogels owing to their unique complex-forming abilities, which have inspired the interesting development of many supramolecular systems for biomedical

Received: April 16, 2014

Accepted: June 11, 2014

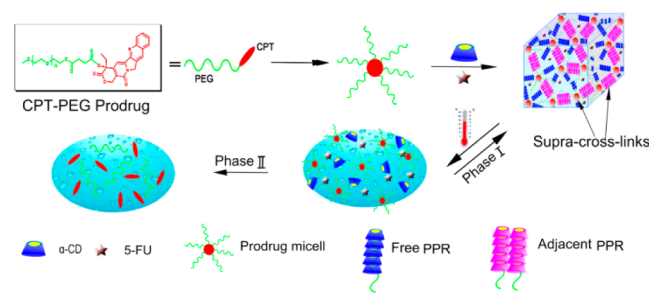
Published: June 11, 2014

and pharmaceutical applications.<sup>35–42</sup> In this area, one of the most well-known assemblies is pseudopolyrotaxane (PPR), formed by a linear polymer chain threading a series of CD cavities. This is a classic and successful model of supramolecular chemistry applied to self-assembly hydrogels. Strong hydrogen bonds between the adjacent threaded CDs result in microcrystalline aggregation and then promote physical gel formation.<sup>43,44</sup> It has been reported that the threading–dethreading process of PPR is a thermosensitive dynamic equilibrium, and the threading–dethreading transition temperature can be affected by the length of PEG chain and concentration of  $\alpha$ -CD,<sup>45,46</sup> which endows the PPR hydrogel with tunable temperature-responsive potentials.

In order to improve the efficiency, reduce side effects, and overcome drug resistance during chemotherapy, anticancer drugs with more than a single component are usually administered in clinics. Therefore, it will be beneficial to develop effective PPR-hydrogel-loading multiple-anticancer drugs as a codelivery system.<sup>47–49</sup> Most PPR hydrogels as drug carriers only load single water-soluble therapeutic agents owing to their highly hydrated, hydrophilic microstructures. Most anticancer drugs, however, have poor water solubility. Therefore, developing PPR hydrogels to load multiple anticancer drugs with diverse physicochemical properties remains a challenge.

In this work, hydrophobic anticancer drug camptothecin (CPT) has been conjugated to a class of low-molecular-weight (MW) poly(ethylene glycol) (PEG) chains (MW = 500, 1000, and 2000), forming an amphiphilic prodrug. After mixing aqueous solutions of the prodrug and  $\alpha$ -CD, supramolecular hydrogels were formed based on a combination of the partial inclusion complexation between one end of the PEG blocks and  $\alpha$ -CD and the hydrophobic aggregation of the CPT groups (Scheme 1). Meanwhile, the formed hydrogels could be loaded

**Scheme 1. Schematic Representation of the Supramolecular PPR Hydrogels and the Temperature-Responsive Dual Phase Drug Release Process**



with water-soluble drug 5-fluorouracil (5-FU), which is always combined with CPT drugs to enhance their anticancer activity. The resulting hydrogels are characterized by possessing dual phase drug release behavior. It is interesting that the 5-FU loaded PPR prodrug hydrogels demonstrate unique structure-related reversible gel–sol transition properties at a certain temperature due to the reversible supramolecular assembly, and the gel–sol transition temperature could be modulated by varying the length of the PEG chain and the concentrations of  $\alpha$ -CD ( $T_{\text{gel-sol}} = 30\text{--}60\text{ }^{\circ}\text{C}$ ), demonstrating the possibility of achieving on-demand gel–sol transitions. Furthermore, the different controlled release profiles of two different anticancer drugs showed significant temperature-dependent properties.

## EXPERIMENTAL SECTION

**Materials.** Methoxypoly(ethylene glycol) (mPEG,  $M_w = 2000, 1000, 500$ ) was purchased from Sigma-Aldrich without further purification.  $\alpha$ -Cyclodextrin ( $\alpha$ -CD) and 4-(dimethylamino) pyridine (DMAP) were purchased from Aladdin Chemical Co. (China). Camptothecin (CPT) was purchased from Sichuan Jiangyuan Natural Products Co. (China). 5-Fluorouracil (5-FU) was kindly given by Lanzhou University.  $N,N'$ -diisopropylcarbodiimide (DIC) were purchased from Shanghai GL Biochem Ltd. (China). Other reagents were analytically pure and used directly without further purification.

**Measurements.**  $^1\text{H}$  NMR spectra were measured on a Bruker AVANCE III-400 spectrometers. The chemical shifts of  $^1\text{H}$  NMR are expressed in parts per million downfield relative to the internal tetramethylsilane ( $\delta = 0$  ppm) or chloroform ( $\delta = 7.26$  ppm). The crystalline changes of the hydrogels were confirmed by X-ray diffraction measurements, which were performed by using Cu  $K\alpha$  irradiation with a PHILIP X'Pert PRO. The rheological behavior of the hydrogels was investigated using a HAKKE RS6000 rotational rheometer. Thermal characteristics of samples were measured with a ZETZSCH Instruments DSC200F3 differential scanning calorimeter. A heating rate of  $2\text{ }^{\circ}\text{C}/\text{min}$  with a temperature range from 10 to  $120\text{ }^{\circ}\text{C}$  was used for DSC. For the scanning electron microscopy (SEM) observations, the specimens were freeze-dried under a vacuum and ground to fine powder. The powder was placed on conducting glue and coated with gold vapor and then analyzed on a JSM-5600LV electron microscope.

**Supramolecular Hydrogelation.** The mPEG-CPT was synthesized in high yield by coupling mPEG-COOH with CPT in the presence of DIC and DMAP according to our reported method (see in the Supporting Information).<sup>47</sup> The general protocol for the hydrogel formation is as follows: An aqueous solution of  $\alpha$ -CD (80.0 mg/mL) was added to an aqueous solution of CPT-PEG500 (G1), CPT-PEG1000 (G2), and CPT-PEG2000 (G3); for all the samples, the concentration of CPT-PEG is 10 mg/mL. At a fixed concentration of CPT-PEG500 (10 mg/mL), various concentrations of  $\alpha$ -CD were used to formulate different hydrogels: 50 mg/mL (G4), 70 mg/mL (G5), 90 mg/mL (G6), and 130 mg/mL (G7). For all the samples, the solution was mixed thoroughly by sonication for 5 min followed by incubation at room temperature for 72 h before measurements. The gelation times of all the hydrogels were estimated through a vial-tilting method. The timing was started immediately after mixing two components until no flow was observed for at least 1 min when a vial containing the hydrogel was inverted. For encapsulating 5-FU,  $\alpha$ -CD and 5.0 mg 5-FU were added to 1.0 mL of an aqueous solution of CPT-PEG (20.0 mg/mL); the solution was mixed thoroughly via sonication for 5 min followed by incubation at room temperature for 72 h before measurements. The encapsulation efficiency and loading efficiency of CPT and 5-FU on supramolecular hydrogels are shown in the Supporting Information (Table S1). The gel–sol transition temperature ( $T_{\text{gel-sol}}$ ) and the reverse sol–gel transition ( $T_{\text{sol-gel}}$ ) were determined using a vial inversion method with a monotonic temperature increase or decrease. Thus, the vials of hydrogel samples were immersed in a water bath at each temperature for 15 min; the  $T_{\text{gel-sol}}$  and  $T_{\text{sol-gel}}$  were monitored visually according to whether the hydrogels flowed when inverting the vials for 1.0 min.

**In Vitro Release Kinetics Studies.** The 5-FU loaded CPT-PEG hydrogels were prepared in a 1.5 mL cuvette. The cuvette was placed upside-down in a test tube with 30.0 mL of phosphate buffered saline (PBS) and incubated in a  $37\text{ }^{\circ}\text{C}$  water bath. The PBS was changed at determined intervals of time. The concentrations of 5-FU and CPT-PEG prodrug released from hydrogels were determined using an Agilent 1260 high performance liquid chromatographic system. Chromatographic separation was performed on an Agilent ZORBAX SB-C18 column ( $4.6 \times 150$  mm,  $5\text{ }\mu\text{m}$ ) at  $30\text{ }^{\circ}\text{C}$  with methanol and 0.1% phosphoric acid aqueous solutions (75:25, v/v) as a mobile phase at a flow rate of 1.0 mL/min. A wavelength of 372 nm was used to detect CPT-PEG and 265 nm to detect 5-FU. The concentrations of CPT-PEG and 5-FU were calculated on the basis of the linear regression equations.

## RESULTS AND DISCUSSION

### Effect of PEG Chain Length on the Gel–Sol Transition Behavior of Temperature Responsive Hydrogel. Table 1

**Table 1.** Preparation of Temperature Responsive Supramolecular Hydrogels

sample	prodrug (mg/mL)	$\alpha$ -CD (mg/mL)	gels	gelation time	$T_{\text{gel-sol}}$ ( $T_{\text{sol-gel}}$ ) ( $^{\circ}\text{C}$ )
CPT-PEG500	10	80	G1	3 h	40 (25)
CPT-PEG1000	10	80	G2	10 min	45 (33)
CPT-PEG2000	10	80	G3	5 min	60 (37)
CPT-PEG500	10	50	G4	48 h	30 (25)
	10	70	G5	5 h	40 (28)
	10	90	G6	10 min	50 (25)
	10	130	G7	5 min	60 (38)

lists the CPT-PEG PPR hydrogel formed between  $\alpha$ -CD and PEG with various MWs. The gelation time for different gels, at an equal concentration of polymer and  $\alpha$ -CD, increased with the decrease of the PEG chain length. This is mainly because  $\alpha$ -CDs are easily dethreaded from short PEG chains, which is unfavorable for PPR formation. All of the hydrogels exhibited a reversible gel–sol transition with increasing or decreasing temperature (Figure 1). They became mobile above a certain

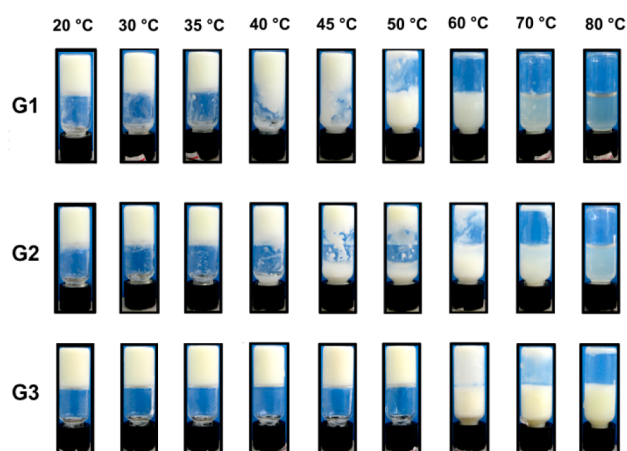


**Figure 1.** Photographs of hydrogels G1, G2, and G3 at different temperatures.

temperature ( $T_{\text{gel-sol}}$ ) and returned to an opaque gel phase after cooling to a certain temperature ( $T_{\text{sol-gel}}$ ). The gel–sol transition temperature ( $T_{\text{gel-sol}}$ ), as expected, lowered with decreasing the length of PEG chains, and G1 is thermosensitive at temperatures close to body temperature, which represents the temperature acceptable for site-specific drug delivery to living cells. This was because the dethreading of  $\alpha$ -CD from a short PEG chain occurs when the polymer chain is more mobile at higher temperatures. For the same reason, such a dethreading process would become more difficult for CPT-PEG blocks with a longer chain length. Hydrogels G1, G2, and G3 showed reversible gel–sol transitions. When  $T < T_{\text{sol-gel}}$ , the opaque hydrogels were formed again, and the inconsistent temperature of  $T_{\text{gel-sol}}$  and  $T_{\text{sol-gel}}$  can be explained by the hysteresis effect.<sup>50</sup>

The thermal behavior of the CPT-PEG hydrogels was further characterized by differential scanning calorimetry (DSC). The DSC thermograms of the hydrogels were obtained by directly heating scans of hydrogels in distilled water. As shown in Figure 2, the hydrogels of G1, G2, and G3 all show an endothermic

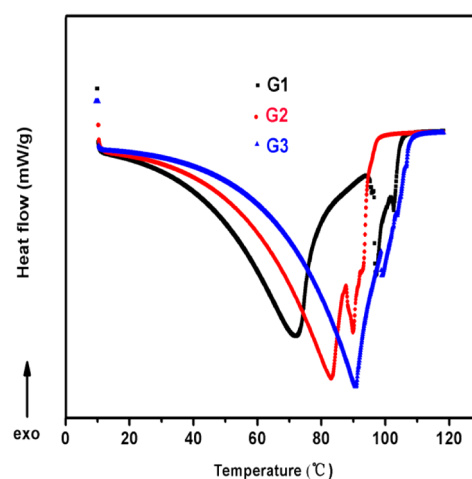


**Figure 2.** DSC thermograms recorded during heating of G1, G2, and G3.

broad peak during heating owing to the phase transition of the PPR in hydrogel to the dissociation state. These observations suggest that the hydrogel network structure is completely homogeneous, and the inclusion complexes between  $\alpha$ -CD and the PEG chain play an important role in forming hydrogels. The dethreading of  $\alpha$ -CD from PEG blocks is an endothermic process; during the heating process, the partial dethreading of  $\alpha$ -CD from adjacent PPR (supra-cross-links) will result in the gel–sol transition of hydrogels. After the hydrogel turned to the sol state, most of the PEG blocks were still covered by  $\alpha$ -CD. Therefore, the peak temperature of the threading–dethreading transition of PPR recorded in Figure 2 is higher than the gel–sol transition temperature of hydrogels recorded in Figure 1. Furthermore, the peak temperature of the threading–dethreading transition of PPR which existed in hydrogels is gradually decreased with shortening the length of PEG chain. This decrease in threading–dethreading transition temperature is probably due to the movability increase of the PEG chain, which improves the self-assembly reversibility of PPR and further promotes the transition of the CPT-PEG PPR hydrogels structure.

To further confirm the effect of the PPR complexes formed between  $\alpha$ -CD and different PEG chains on the formation of hydrogels, complementary XRD studies were carried out to give additional information on their nanoscale structure (Figure 3). For a comparison, pure  $\alpha$ -CD and pure CPT-PEG (the XRD pattern of CPT-PEG500, CPT-PEG1000, and CPT-PEG2000 are the same) were also measured. The sharp diffraction peak at  $2\theta = 19.8^{\circ}$  (G1, G2, and G3) is identical with the extended channel structure of  $\alpha$ -CD, which corresponds to the crystalline  $\alpha$ -CD-PEG inclusion complexes.<sup>36,51</sup> Two weak and broad peaks (11.5 and 23) associated with the random structure of  $\alpha$ -CD exist in G1, G2, and G3, which indicates that both complexed and uncomplexed  $\alpha$ -CD exist in the gel systems.

The introduction of various PEG chains shows remarkable effects not only on the thermoresponsive behavior but also on

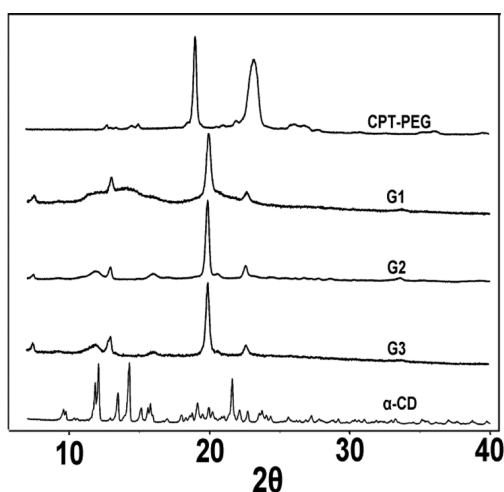


Figure 3. X-ray diffraction patterns for dried  $\alpha$ -CD, pure CPT-PEG, G1, G2, and G3.

the strength and viscosity of the hydrogels. Figures S7–S9 show the dynamic stress sweep data of G1–G3. As shown in Figures S7–S9, the values of the storage modulus ( $G'$ ) and the loss modulus ( $G''$ ) exhibit a weak dependence of stress, indicating that all samples are viscoelastic. As shown in Figure 4, at a fixed stress, both the storage modulus ( $G'$ ) and the viscosity of the hydrogels increased with an increase in PEG chain length. For example, the  $G'$  of the CPT-PEG2000

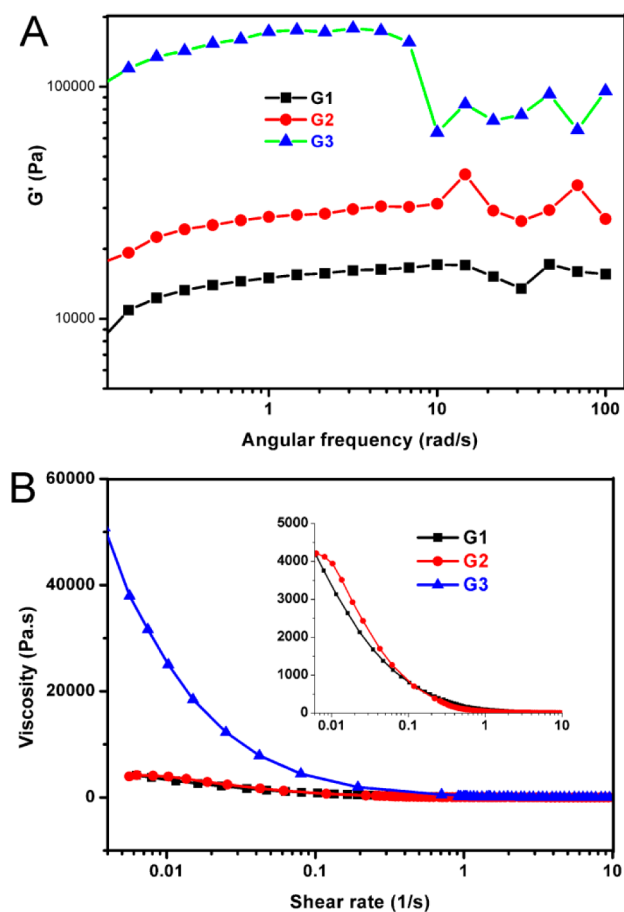


Figure 4. (A) Dynamic and (B) steady rheological behaviors of G1, G2, and G3.

hydrogel (G3) is  $\sim 10$  times higher than that of CPT-PEG500 (G1) over a broad frequency range. Meanwhile, the viscosity of G3 at a low shear rate reaches  $\sim 50000$  Pa·s, whereas that of G1 is only  $\sim 4000$  Pa·s. Such a difference in the rheological behavior, we believed, is also attributed to the stability of PPR with different PEG chain lengths. More importantly, all CPT-PEG hydrogel exhibits good shear-thinning behavior, a basic and valuable property required for injectable hydrogels.<sup>24</sup> This shear-thinning effect can be attributed to the supra-cross-links. Under shearing, both the micelles of the CPT-PEG prodrug in the hydrogels and the PPR between the PEG chain and  $\alpha$ -CD would be partially dissociated, leading to a substantial decrease in the degree of cross-links.

The morphology of the hydrogels was observed by SEM. And for a comparison, the crystalline complexes formed by  $\alpha$ -CD and mPEG were also examined. As shown in Figure 5, the

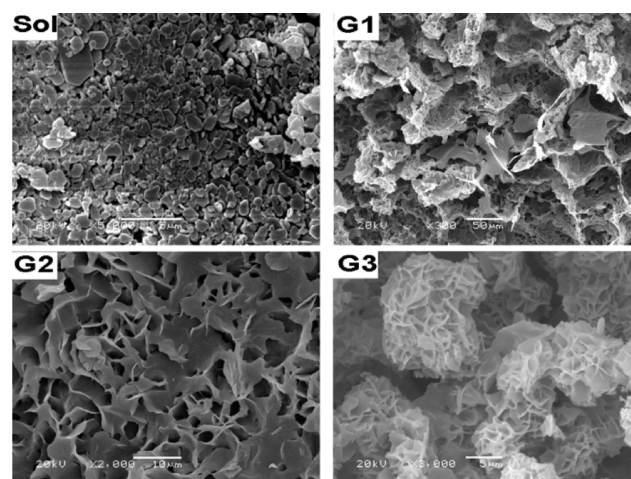


Figure 5. SEM images of the crystal complex made of  $\alpha$ -CD and mPEG (Sol) and G1, G2, and G3.

complexes show a typical disk-like crystalline structure (Sol), whereas all the obtained hydrogels clearly demonstrate the presences of a typical porous structure (G1, G2, and G3). The existence of such a porous structure is indispensable in biomedical applications, such as tissue engineering and drug delivery, allowing for tissue growth and diffusion of drugs and nutrients.<sup>52–54</sup> Moreover, a higher percentage of pore fractions and smaller pore size were obtained by increasing the PEG chain, which might be due to the increase of network density.

**Effect of  $\alpha$ -CD Concentration on the Gel–Sol Transition Behavior of Temperature Responsive Hydrogel.** Besides the PEG chain length, the effect of  $\alpha$ -CD concentration on the gel–sol transition temperature of PPR hydrogels was also evaluated. Table 1 lists the CPT-PEG500 PPR hydrogel formed between CPT-PEG500 and  $\alpha$ -CD at different concentrations. The gelation time for different gels, at equal concentrations of polymer, dramatically increased with decreasing of the  $\alpha$ -CD concentration. It has been reported that the formation process of PPR could be divided into five different steps: (1) diffusion of  $\alpha$ -CD and PEG blocks in the solvent, (2) initial threading of PEG ends into  $\alpha$ -CD cavities, (3) sliding of  $\alpha$ -CD over the PEG chain, (4) dethreading of  $\alpha$ -CD from the PEG chain, and (5) precipitation of the final PPR.<sup>46</sup> It could be found that the formation of PPR is a dynamic equilibrium, the key factor of which is the concentration of  $\alpha$ -CD. When the amount of  $\alpha$ -CD in the

solutions exceeds a certain value, step 4 cannot occur easily; thus the PPR forms. However, at low concentrations of  $\alpha$ -CD, step 4 can be easily undertaken; thus, the gel time prolongs.

The hydrogels G4–G7 also exhibited a reversible gel–sol transition with increasing or decreasing temperature (Figure 6).

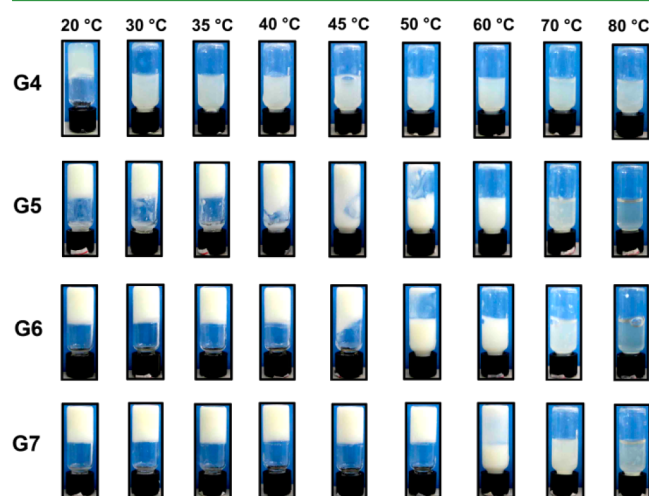


**Figure 6.** Photographs of hydrogels G4, G5, G6, and G7 at different temperature.

The  $T_{\text{gel-sol}}$  as expected, decreased with the decrease of  $\alpha$ -CD concentration and can be modulated ranging from 30 to 60 °C by adding different amount of CDs, which particularly provides more flexible applications for hydrogels.

Complementary XRD was carried out to further investigate the effect of  $\alpha$ -CD concentration on nanoscale structure of different hydrogels (Figure 7). The sharp diffraction peak at  $2\theta$

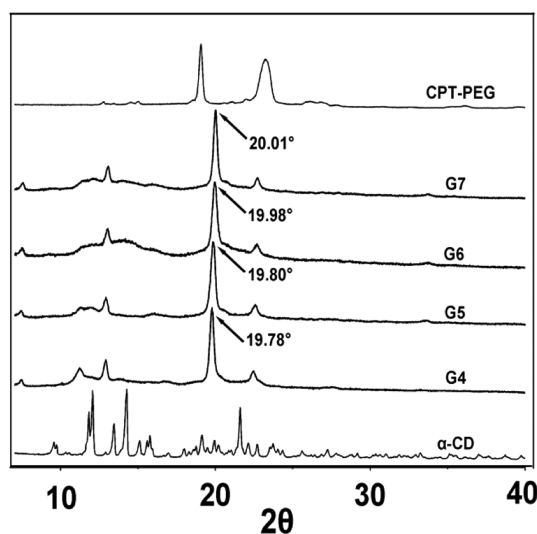


**Figure 7.** X-ray diffraction patterns for dried  $\alpha$ -CD, pure CPT-PEG, G4, G5, G6, and G7.

= 19.8–20.0° (G4, G5, G6, and G7) is consistent with the extended channel structure of  $\alpha$ -CD, which corresponds to the crystalline  $\alpha$ -CD-PEG inclusion complexes. Furthermore, it is worth noting that the diffraction peak position ( $2\theta$ ) of  $\alpha$ -CD-PEG inclusion complexes in different hydrogels slightly increased with increasing the concentration of  $\alpha$ -CD (Figure 7, G4–G7). Such an increase may be due to the fact that more

CDs could be included into the PEG chains in the formation process of hydrogels when  $\alpha$ -CD at higher concentrations is used.

As PEG chain length displayed, the introduction of different amounts of CDs also demonstrated a significant change for the rheological behavior of the hydrogels. As shown in Figure 8,

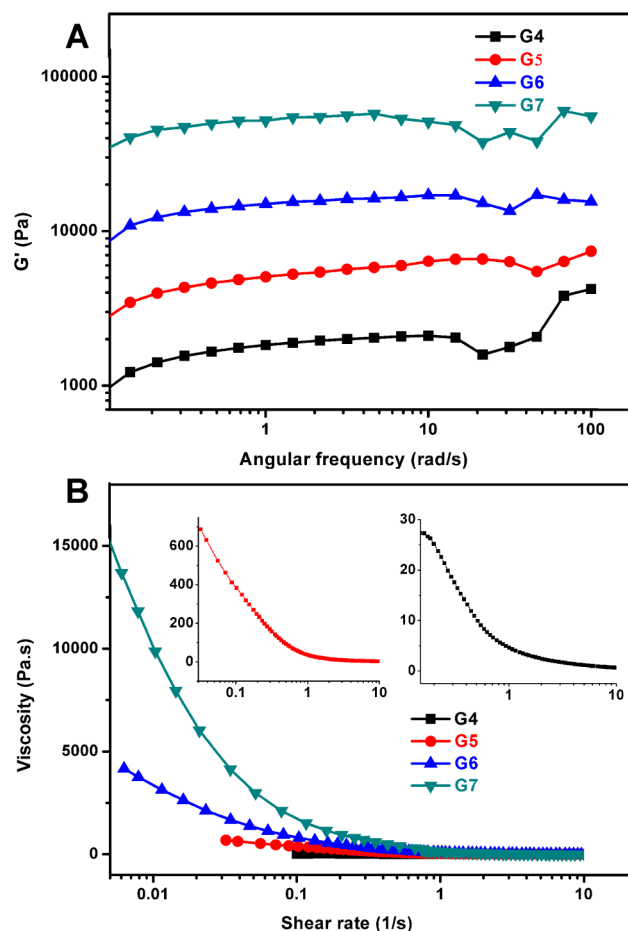


**Figure 8.** (A) Dynamic and (B) steady rheological behaviors of G4, G5, G6, and G7.

both the storage modulus ( $G'$ ) and the viscosity of the hydrogels dramatically increased with increasing the  $\alpha$ -CD concentration. For example, the  $G'$  of the G7 is  $\sim 30$  times higher than that of G4 over a broad frequency range while the concentration of  $\alpha$ -CD increased only  $\sim 3$  times. Meanwhile, all the CPT-PEG500 hydrogels also show good shear-thinning behavior. As the concentration of  $\alpha$ -CD increases during the forming process of hydrogels, the amount of  $\alpha$ -CD included into the PEG chain would increase correspondingly, which subsequently increases the density of the network and stability of supra-cross-links. The SEM observation further confirmed this effect. As shown in Figure 9, from G4 to G6, the pore size distributions narrowed with increasing  $\alpha$ -CD concentration. The results also revealed cross-linking density increased with increasing  $\alpha$ -CD concentration, which might be attributed to the increase of PPR numbers existing in hydrogels. Furthermore, the morphology of G7 displays a relatively compact gel structure in which the typical porous structure could not be found anymore at higher  $\alpha$ -CD concentration.

On the basis of the above results, we may conclude that the reversible gel–sol transition properties of CPT-PEG PPR

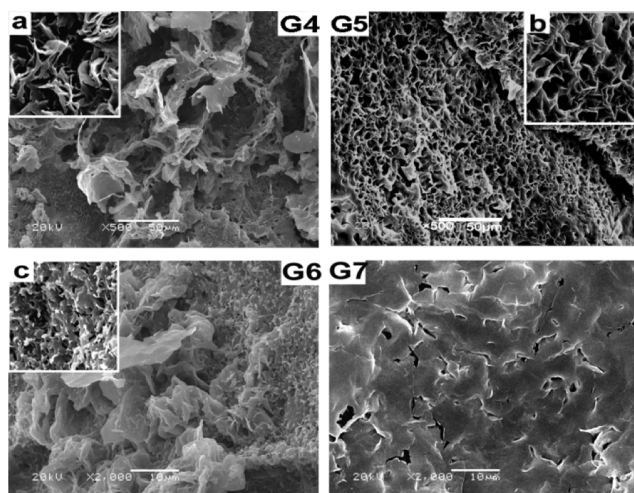


**Figure 9.** SEM images of the G4, G5, G6 and G7. a, b, and c are partial enlarged images of G4, G5, and G6.

hydrogel are closely related to the microstructure of PPR formed during the hydrogel preparation. The number of PPRs formed between  $\alpha$ -CD and the CPT-PEG block, the cover density of  $\alpha$ -CD in PPR, the stability of PPR, and the hydrogen-bond interaction among adjacent PPRs all play an important role in providing the possibility of achieving on-demand gel–sol transition. Varying the length of the PEG and concentration of  $\alpha$ -CD could control over the structure of PPR, which result in tunable mechanical strength, morphology of hydrogels, and reversible gel–sol transition behavior in an independent manner.

**In Vitro Dual-Phase Drug Release Behavior.** The hydrogels were further utilized for encapsulation of another water-soluble anticancer drug 5-fluorouracil (5-FU), which could produce synergetic cytotoxicity with CPT to cancer cells.<sup>47</sup> All the hydrogels demonstrated a structure-related dual phase behavior (Figure 10). In the first stage, the hydrogels showed a controlled release property, sustaining the release of 5-FU accompanied by some release of the CPT-PEG drug. Such release behavior was mainly caused by diffusion and the breakup of the supra-cross-links, which are formed by strong

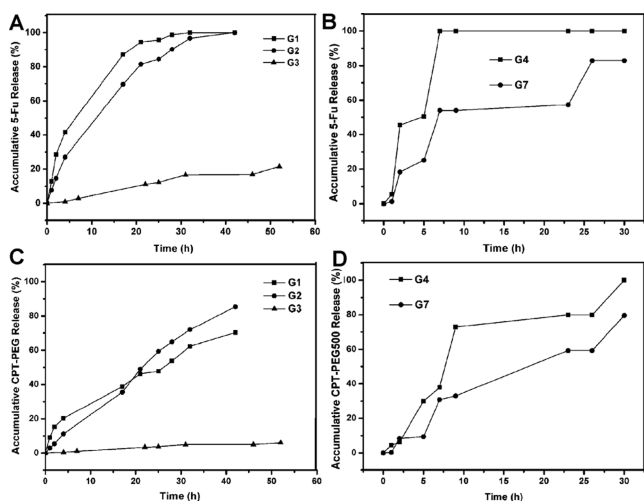


**Figure 10.** 5-FU and CPT-PEG prodrug release kinetics from the CPT-PEG/ $\alpha$ -CD hydrogels in PBS at pH 7.4 and 37 °C.

hydrogen-bond interactions among adjacent rod channel type crystalline structures of PEG- $\alpha$ -CD (Scheme 1). The influence of the PEG chain length and  $\alpha$ -CD concentration on the release of 5-FU and CPT-PEG prodrug can be well explained by the structure of corresponding hydrogels. As shown in Figure 10, upon increasing the PEG chain length (Figure 10A,C) and  $\alpha$ -CD concentration (Figure 10B,D), the diffusion rate of the encapsulated 5-FU and the breakup of supra-cross-links decreased, which could be attributed to the fact the pores become smaller and the network density as well as the mechanical strength of the hydrogels increases. Furthermore, the controlled release profiles of 5-FU and CPT-PEG prodrug also showed significant temperature-dependent properties. As shown in Figure 10B, the drug release rate of 5-FU in G4 is obviously faster than that in G7. This is because G4 would transform into sol at 37 °C, which dramatically accelerates the release rate of encapsulated 5-FU. Therefore, temperature can be used as a switch to trigger the drug release in this system. In the second stage, the CPT-PEG prodrug micelles released from the hydrogel also possessed the ability of releasing CPT via hydrolysis of CPT-PEG (Scheme 1). It has been reported that CPT-PEG would be quickly hydrolyzed and release CPT in the presence of esterase, which is abundant in cytoplasm.<sup>45,55</sup> Such dual phase drug release behavior seems to be generally feasible for drug combination with improved therapeutic windows.

## CONCLUSIONS

In summary, we successfully developed a codelivery PPR hydrogel system composed of CPT-PEG prodrug and  $\alpha$ -CD. By varying the length of the PEG and concentration of  $\alpha$ -CD, the structure of PPR could be under control, resulting in tunable mechanical strength, morphology, and temperature-responsive gel–sol transition behavior in an independent manner. Such a flexible design provides the possibility of achieving on-demand gel–sol transition in many technological applications including biomedical ones. Meanwhile, the formed hydrogels could load water-soluble 5-FU which is always combined with CPT to enhance their anticancer activity. The 5-FU loaded hydrogels delivered two anticancer drugs by structure-related dual phase drug release behavior. In addition, the loaded hydrogels displayed a tunable temperature-responsive gel–sol transition which leads to a dramatic temperature-responsive drug release behavior, suggesting the opportunity of applying this novel drug delivery system for site-specific delivery of drugs using changes in temperature as a trigger.

## ASSOCIATED CONTENT

### Supporting Information

Synthesis route for the CPT-PEG prodrug with various PEG molecular weight; <sup>1</sup>H NMR and <sup>13</sup>C NMR of CPT-mPEG500, CPT-mPEG1000, and CPT-mPEG2000; the encapsulation efficiency and loading efficiency of CPT and 5-FU on supramolecular hydrogels; and the dynamic stress sweep results of G1–G3. This material is available free of charge via the Internet at <http://pubs.acs.org>.

## AUTHOR INFORMATION

### Corresponding Author

\*E-mail: shiyp@licp.cas.cn.

### Notes

The authors declare no competing financial interest.

## ACKNOWLEDGMENTS

The work was supported by the National Nature Science Foundation of China (Nos. 21105106 and 21375136).

## REFERENCES

- (1) Dong, S. Y.; Luo, Y.; Yan, X. Z.; Zheng, B.; Ding, X.; Yu, Y. H.; Ma, Z.; Zhao, Q. L.; Huang, F. H. A Dual-Responsive Supramolecular Polymer Gel Formed by Crown Ether Based Molecular Recognition. *Angew. Chem.* **2011**, *123*, 1945–1949.
- (2) Wang, F.; Zhang, J. Q.; Ding, X.; Dong, S. Y.; Liu, M.; Zheng, B.; Li, S. J.; Wu, L.; Yu, Y. H.; Gibson, H. W.; Huang, F. H. Metal Coordination Mediated Reversible Conversion between Linear and Cross-Linked Supramolecular Polymers. *Angew. Chem.* **2010**, *122*, 1108–1112.
- (3) Liu, Y.; Yu, Y.; Gao, J.; Wang, Z.; Zhang, X. Water-Soluble Supramolecular Polymerization Driven by Multiple Host-Stabilized Charge-Transfer Interactions. *Angew. Chem.* **2010**, *122*, 6726–6729.
- (4) Alarcón, C.; de las, H.; Pennadam, S.; Alexander, C. Stimuli responsive Polymers for Biomedical Applications. *Chem. Soc. Rev.* **2005**, *34*, 276–285.
- (5) Mura, S.; Nicolas, J.; Couvreur, P. Stimuli-responsive Nanocarriers for Drug Delivery. *Nat. Mater.* **2013**, *12*, 991–1003.
- (6) Yin, Q.; Shen, J. N.; Zhang, Z. W.; Yu, H. J.; Li, Y. P. Reversal of Multidrug Resistance by Stimuli-responsive Drug Delivery Systems for Therapy of Tumor. *Adv. Drug Delivery Rev.* **2013**, *65*, 1699–1715.
- (7) Ganta, S.; Devalapally, H.; Shahiwal, A.; Amiji, M. A Review of Stimuli-responsive Nanocarriers for Drug and Gene Delivery. *J. Controlled Release* **2008**, *123*, 187–204.
- (8) Du, J. Z.; Tang, Y. Q.; Lewis, A. L.; Armes, S. P. pH-sensitive Vesicles Based on a Biocompatible Zwitterionic Diblock Copolymer. *J. Am. Chem. Soc.* **2005**, *127*, 17982–17983.
- (9) Saito, G.; Swanson, J. A.; Lee, K. D. Drug Delivery Strategy Utilizing Conjugation via Reversible Disulfide Linkages: Role and Site of Cellular Reducing Activities. *Adv. Drug Delivery Rev.* **2003**, *55*, 199–215.
- (10) Meng, F. H.; Hennink, W. E.; Zhong, Z. Y. Reduction-sensitive Polymers and Bioconjugates for Biomedical Applications. *Biomaterials* **2009**, *30*, 2180–2198.
- (11) Alvarez-Lorenzo, C.; Bromberg, L.; Concheiro, A. Light-sensitive Intelligent Drug Delivery Systems. *Photochem. Photobiol.* **2009**, *85*, 848–860.
- (12) Wei, H.; Cheng, S. X.; Zhang, X. Z.; Zhuo, R. X. Thermo-sensitive Polymeric Micelles Based on Poly(N-isopropylacrylamide) as Drug Carriers. *Prog. Polym. Sci.* **2009**, *34*, 893–910.
- (13) Sun, C.; Lee, J. S. H.; Zhang, M. Magnetic Nanoparticles in MR Imaging and Drug Delivery. *Adv. Drug Delivery Rev.* **2008**, *60*, 1252–1265.
- (14) Lee, J. H.; Oh, H.; Baxa, U.; Raghavan, S. R.; Blumenthal, R. Biopolymer-connected Liposome Networks as Injectable Biomaterials Capable of Sustained Local Drug Delivery. *Biomacromolecules* **2012**, *13*, 3388–3394.
- (15) Xue, Z. X.; Wang, S. T.; Lin, L.; Chen, L.; Liu, M. J.; Feng, L.; Jiang, L. A Novel Superhydrophilic and Underwater Superoleophobic Hydrogel-coated Mesh for Oil/water Separation. *Adv. Mater.* **2011**, *23*, 4270–4273.
- (16) Lee, E.; Kim, B. Smart Delivery System for Cosmetic Ingredients Using pH-sensitive Polymer Hydrogel Particles. *Korean J. Chem. Eng.* **2011**, *28*, 1347–1350.
- (17) Van Vlierberghe, S.; Dubruel, P.; Schacht, E. Biopolymer-based Hydrogels as Scaffolds for Tissue Engineering Application: A Review. *Biomacromolecules* **2011**, *12*, 1387–1400.
- (18) Hoffman, A. S. Hydrogels for Biomedical Applications. *Adv. Drug Delivery Rev.* **2002**, *54*, 3–12.
- (19) Slaughter, B. V.; Khurshid, S. S.; Fisher, O. Z.; Khademhosseini, A.; Peppas, N. A. Hydrogels in Regenerative Medicine. *Adv. Mater.* **2009**, *21*, 3307–3329.
- (20) Zhou, C.; Hillmyer, M. A.; Lodge, T. P. Efficient Formation of Multicompartment Hydrogels by Stepwise Self-Assembly of Thermoresponsive ABC Triblock Terpolymers. *J. Am. Chem. Soc.* **2012**, *134*, 10365–10368.
- (21) Buenger, D.; Topuz, F.; Groll, J. Hydrogels in Sensing Applications. *Prog. Polym. Sci.* **2012**, *37*, 1678–1719.
- (22) He, C.; Kim, S. W.; Lee, D. S. In situ Gelling Stimuli-sensitive Block Copolymer Hydrogels for Drug Delivery. *J. Controlled Release* **2008**, *127*, 189–207.
- (23) Gil, E. S.; Hudson, S. M. Stimuli-responsive Polymers and Their Bioconjugates. *Prog. Polym. Sci.* **2004**, *29*, 1173–1222.
- (24) Jeong, B.; Kim, S. W.; Bae, Y. H. Thermosensitive Sol-gel Reversible Hydrogels. *Adv. Drug Delivery Rev.* **2012**, *64* (Supplement), 154–162.
- (25) Moon, H. J.; Ko, D. Y.; Park, M. H.; Joo, M. K.; Jeong, B. Temperature-responsive Compounds as In situ Gelling Biomedical Materials. *Chem. Soc. Rev.* **2012**, *41*, 4860–4883.
- (26) Zhang, Z. X.; Liu, K. L.; Li, J. A. Thermoresponsive Hydrogel Formed from a Star-Star Supramolecular Architecture. *Angew. Chem.* **2013**, *125*, 6300–6304.
- (27) O'Lenick, T. G.; Jiang, X. G.; Zhao, B. Thermosensitive Aqueous Gels with Tunable Sol-Gel Transition Temperature from Thermo- and pH-Responsive Hydrophilic ABA Triblock Copolymer. *Langmuir* **2010**, *26*, 8787–8796.
- (28) Chopko, C. M.; Lowden, E. L.; Engler, A. C.; Griffith, L. G.; Hammond, P. T. Dual Responsiveness of a Tunable Thermosensitive Polypeptide. *ACS Macro. Lett.* **2012**, *1*, 727–731.
- (29) Gu, X.; Wang, J. J.; Liu, X. F.; Zhao, D. P.; Wang, Y. N.; Gao, H.; Wu, G. L. Temperature-responsive Drug Delivery Systems Based on Polyaspartamides with Isopropylamine Pendant Groups. *Soft Matter* **2013**, *9*, 7267–7273.
- (30) Hwang, I.; Jeon, W. S.; Kim, H. J.; Kim, D. W.; Kim, H.; Selfapalang, N.; Fujita, N.; Shinkai, S.; Kim, K. Cucurbit[7]uril: A Simple Macrocyclic, pH-Triggered Hydrogelator Exhibiting Guest-Induced Stimuli-Responsive Behavior. *Angew. Chem.* **2007**, *46*, 210–213.
- (31) Hoare, T. R.; Kohane, D. S. Hydrogels in Drug Delivery: Progress and Challenges. *Polymer* **2008**, *49*, 1993–2007.
- (32) Komatsu, H.; Matsumoto, S.; Tamaru, S. I.; Kaneko, K.; Ikeda, M.; Hamachi, I. Supramolecular Hydrogel Exhibiting Four Basic Logic Gate Functions to Fine-Tune Substance Release. *J. Am. Chem. Soc.* **2009**, *131*, 5580–5585.
- (33) Sivakova, S.; Bohnsack, D. A.; Mackay, M. E.; Suwanmala, P.; Rowan, S. J. Utilization of a Combination of Weak Hydrogen-Bonding Interactions and Phase Segregation to Yield Highly Thermosensitive Supramolecular Polymers. *J. Am. Chem. Soc.* **2005**, *127*, 18202–18211.
- (34) Smith, D. K. Lost in Translation? Chirality Effects in The Self-assembly of Nanostructures Gel-phase Materials. *Chem. Soc. Rev.* **2009**, *38*, 684–694.
- (35) Li, J.; Yang, C.; Li, H.; Wang, X.; Goh, S. H.; Ding, J. L.; Wang, D. Y.; Leong, K. W. Cationic Supramolecules Composed of Multiple Oligoethylenimine-Grafted  $\beta$ -Cyclodextrins Threaded on a Polymer Chain for Efficient Gene Delivery. *Adv. Mater.* **2006**, *18*, 2969–2974.
- (36) Li, J.; Li, X.; Ni, X. P.; Wang, X.; Li, H. Z.; Leong, K. W. Self-assembled Supramolecular Hydrogels Formed by Biodegradable PEO-PHB-PEO Triblock Copolymers and  $\alpha$ -cyclodextrin for Controlled Drug Delivery. *Biomaterials* **2006**, *27*, 4132–4140.
- (37) Ogoshi, T.; Takashima, Y.; Yamaguchi, H.; Harada, A. Chemically-Responsive Sol–Gel Transition of Supramolecular Single-Walled Carbon Nanotubes (SWNTs) Hydrogel Made by Hybrids of SWNTs and Cyclodextrins. *J. Am. Chem. Soc.* **2007**, *129*, 4878–4879.
- (38) Liu, J. H.; Chen, G. S.; Guo, M. Y.; Jiang, M. Dual Stimuli-Responsive Supramolecular Hydrogel Based on Hybrid Inclusion Complex (HIC). *Macromolecules* **2010**, *43*, 8086–8093.
- (39) Liao, X. J.; Chen, G. S.; Liu, X. X.; Chen, W. X.; Chen, F. E.; Jiang, M. Photoresponsive Pseudopolyrotaxane Hydrogels Based on Competition of Host-Guest Interactions. *Angew. Chem., Int. Ed.* **2010**, *49*, 4409–4413.

- (40) Liu, J. H.; Chen, G. S.; Jiang, M. Supramolecular Hybrid Hydrogels from Noncovalently Functionalized Graphene with Block Copolymers. *Macromolecules* **2011**, *44*, 7682–7691.
- (41) Du, P.; Liu, J. H.; Chen, G. S.; Jiang, M. Dual Responsive Supramolecular Hydrogel with Electrochemical Activity. *Langmuir* **2011**, *27*, 9602–9608.
- (42) Chen, G. S.; Jiang, M. Cyclodextrin-based Inclusion Complexation Bridging Supramolecular Chemistry and Macromolecular Self-assembly. *Chem. Soc. Rev.* **2011**, *40*, 2254–2266.
- (43) Li, J.; Loh, X. J. Cyclodextrin-based Supramolecular Architectures: Syntheses, Structures, and Applications for Drug and Gene Delivery. *Adv. Drug Delivery Rev.* **2008**, *60*, 1000–1017.
- (44) Harada, A.; Hashidzume, A.; Yamaguchi, H.; Takashima, Y. Polymeric Rotaxanes. *Chem. Rev.* **2009**, *109*, 5974–6023.
- (45) Li, J.; Ni, X.; Leong, K. W. Injectable Drug-delivery Systems Based on Supramolecular Hydrogels Formed by Poly(ethylene oxide)s and  $\alpha$ -cyclodextrin. *J. Biomed. Mater. Res.* **2003**, *65A*, 196–202.
- (46) Ceccato, M.; Nostro, P. L.; Baglioni, P.  $\alpha$ -Cyclodextrin/Polyethylene Glycol Polyrotaxane: A Study of the Threading Process. *Langmuir* **1997**, *13*, 2436–2439.
- (47) Ha, W.; Yu, J.; Song, X. Y.; Zhang, Z. J.; Liu, Y. Q.; Shi, Y. P. Prodrugs Forming Multifunctional Supramolecular Hydrogels for Dual Cancer Drug Delivery. *J. Mater. Chem. B* **2013**, *1*, 5532–5538.
- (48) Mao, L. N.; Wang, H. M.; Tan, M.; Ou, L. L.; Kong, D. L.; Yang, Z. M. Conjugation of Two Complementary Anti-cancer Drugs Confers Molecular Hydrogels as a Co-delivery System. *Chem. Commun.* **2012**, *48*, 395–397.
- (49) Wang, H. M.; Yang, Z. M. Molecular Hydrogels of Hydrophobic Compounds: a Novel Self-delivery System for Anti-cancer Drugs. *Soft Matter* **2012**, *8*, 2344–2347.
- (50) Huh, K. M.; Ooya, T.; Lee, W. K.; Sasaki, S.; Kwon, I. C.; Jeong, S. Y.; Yui, N. Supramolecular-Structured Hydrogels Showing a Reversible Phase Transition by Inclusion Complexation between Poly(ethylene glycol) Grafted Dextran and  $\alpha$ -Cyclodextrin. *Macromolecules* **2001**, *34*, 8657–8662.
- (51) Li, J.; Li, X.; Zhou, Z.; Ni, X.; Leong, K. W. Formation of Supramolecular Hydrogels Induced by Inclusion Complexation between Pluronic and  $\alpha$ -Cyclodextrin. *Macromolecules* **2001**, *34*, 7236–7237.
- (52) He, J. L.; Zhang, M. Z.; Ni, P. H. Rapidly in situ Forming Polyphosphoester-based Hydrogels for Injectable Drug Delivery Carriers. *Soft Matter* **2012**, *8*, 6033–6038.
- (53) Gopishetty, V.; Tokarev, I.; Minko, S. Biocompatible Stimuli-responsive Hydrogel Porous Membranes via Phase separation of a Polyvinyl Alcohol and Na-alginate Intermolecular Complex. *J. Mater. Chem.* **2012**, *22*, 19482–19487.
- (54) Bertz, A.; Wöhl-Bruhn, S.; Miethe, S.; Tiersch, B.; Koetz, J.; Hust, M.; Bunjes, H.; Menzel, H. Encapsulation of Proteins in Hydrogel Carrier Systems for Controlled Drug Delivery: Influence of Network Structure and Drug Size on Release Rate. *J. Biotechnol.* **2013**, *163*, 243–249.
- (55) Shen, Y. Q.; Jin, E.; Zhang, B.; Murphy, C. J.; Sui, M. H.; Zhao, J.; Wang, J. Q.; Tang, J. B.; Fan, M. H.; Kirk, E. V.; Murdoch, W. J. Prodrugs Forming High Drug Loading Multifunctional Nanocapsules for Intracellular Cancer Drug Delivery. *J. Am. Chem. Soc.* **2010**, *132*, 4259–4265.